

The consequence of an additional NADH dehydrogenase paralog on the growth of *Gluconobacter oxydans* DSM3504

D. Kostner · B. Luchterhand · A. Junker · S. Volland ·
R. Daniel · J. Büchs · W. Liebl · A. Ehrenreich

Received: 20 June 2014 / Revised: 29 August 2014 / Accepted: 2 September 2014 / Published online: 30 September 2014
© Springer-Verlag Berlin Heidelberg 2014

Abstract Acetic acid bacteria such as *Gluconobacter oxydans* are used in several biotechnological processes due to their ability to perform rapid incomplete regio- and stereo-selective oxidations of a great variety of carbohydrates, alcohols, and related compounds by their membrane-bound dehydrogenases. In order to understand the growth physiology of industrial strains such as *G. oxydans* ATCC 621H that has high substrate oxidation rates but poor growth yields, we compared its genome sequence to the genome sequence of strain DSM 3504 that reaches an almost three times higher optical density. Although the genome sequences are very similar, DSM 3504 has additional copies of genes that are absent from ATCC 621H. Most importantly, strain DSM 3504 contains an additional type II NADH dehydrogenase (*ndh*) gene and an additional triosephosphate isomerase (*tpi*) gene. We deleted these additional paralogs from DSM 3504, overexpressed NADH dehydrogenase in ATCC 621H, and monitored biomass and the concentration of the representative cell components as well as O₂ and CO₂ transfer rates in

growth experiments on mannitol. The data revealed a clear competition of membrane-bound dehydrogenases and NADH dehydrogenase for channeling electrons in the electron transport chain of *Gluconobacter* and an important role of the additional NADH dehydrogenase for increased growth yields. The less active the NADH dehydrogenase is, the more active is the membrane-bound polyol dehydrogenase. These results were confirmed by introducing additional *ndh* genes via plasmid pAJ78 in strain ATCC 621H, which leads to a marked increase of the growth rate.

Keywords *Gluconobacter* · Acetic acid bacteria · Growth · NADH dehydrogenase · Membrane-bound dehydrogenases · Electron transport chain · RAMOS

Introduction

The acetic acid bacterium *Gluconobacter oxydans* is often employed in oxidative fermentations due to its ability to perform incomplete oxidations of various sugars, sugar alcohols, and sugar acids (De Muyne et al. 2007). *G. oxydans* is used for the production of L-sorbose, D-gluconic acid, dihydroxyacetone, and precursors of vitamin C and in many other biotechnological processes (Gupta et al. 2001). The oxidation reactions are catalyzed by numerous membrane-bound dehydrogenases that are linked directly to the respiratory chain (Matsushita et al. 1994). The catalytic centers of the enzymes are oriented toward the periplasm; therefore, the resulting products accumulate directly in the medium, which facilitates product recovery enormously (Deppenmeier et al. 2002). The stereo- and regio-specific oxidation capabilities of these membrane-bound dehydrogenases allow the production of enantiomerically pure compounds that are hard or not at all obtainable by chemical methods (Schweiger et al. 2007). The determination of the genome sequence of *G. oxydans* ATCC

Electronic supplementary material The online version of this article (doi:10.1007/s00253-014-6069-9) contains supplementary material, which is available to authorized users.

D. Kostner · A. Junker · W. Liebl · A. Ehrenreich (✉)
Lehrstuhl für Mikrobiologie, Technische Universität München,
Emil-Ramann Str. 4, 85354 Freising, Germany
e-mail: aehrenr@mikro.biologie.tu-muenchen.de

S. Volland · R. Daniel
Department of Genomic and Applied Microbiology & Göttingen
Genomics Laboratory, Georg-August University Göttingen,
Göttingen, Germany

B. Luchterhand · J. Büchs
Department of Biochemical Engineering, RWTH Aachen University,
Aachen, Germany

621H (Prust et al. 2005) offered the possibility to investigate many characteristics of this biotechnologically relevant strain at the genome level (Deppenmeier and Ehrenreich 2009). The strain ATCC 621H is characterized by high substrate oxidation rates due to the very active membrane-bound dehydrogenases, which qualifies it as an industrial production strain despite the disadvantage of low biomass production (Prust et al. 2005). Therefore, a possibility to boost the growth yield would increase the productivity and lead to an improved profitability of many processes.

The strain *G. oxydans* DSM 3504 was originally identified as an efficient producer of 2-keto-L-gluconic acid (Motizuki et al. 1966). In contrast to strain ATCC 621H, the growth yields of strain DSM 3504 are significantly higher (Elfari et al. 2005). We sequenced the genome of strain DSM 3504 and compared it to the genome of strain ATCC 621H in order to elucidate the differing growth characteristics of these two closely related organisms. As we have developed an efficient markerless in-frame deletion system for *G. oxydans* strains (Kostner et al. 2013), we constructed several deletion mutants of strain DSM 3504 in order to analyze the role of prominent differing genes with potential influence on growth characteristics. In various growth experiments with different deletion mutants of strain DSM 3504 and with strain ATCC 621H containing the plasmid pAJ78 expressing an additional *ndh* gene, we recognized that the additional copy of a type II NADH dehydrogenase (NDH-2) is of major importance for the improved growth of *G. oxydans* DSM 3504. The results were obtained by exact online measurements of generated biomass, NADH and FAD concentrations, and O₂ and CO₂ transfer rates using BioLector system (Samorski et al. 2005) and Respiration Activity Monitoring System (RAMOS) (Anderlei et al. 2004) as well as off-line determination of substrate consumption by HPLC.

Materials and methods

Chemicals

Yeast extract and peptone were obtained from Carl Roth (Karlsruhe, Germany), 5-fluorocytosine (FC) from TCI Europe N.V. (Zwijndrecht, Belgium), kanamycin (Km) from AppliChem (Darmstadt, Germany), and mannitol, cefoxitin (Cef), FU, and other chemicals were purchased from Sigma-Aldrich (Steinheim, Germany).

Bacterial strains and culture methods

Escherichia coli TOP10 was purchased from Invitrogen (Karlsruhe, Germany) and grown in LB Medium at 37 °C in 250-mL shaking flasks and 180 rpm on a rotary shaker from Infors HT Modell Orbitron (Bottmingen, Switzerland)

(Sambrook et al. 1989). The strains *G. oxydans* ATCC 621H (DSM 2343) and DSM 3504 were obtained from Deutsche Sammlung von Mikroorganismen und Zellkulturen (Braunschweig, Germany) and were grown in mannitol standard medium containing 5 g/L yeast extract, 3 g/L peptone, and 50 mM mannitol, pH 6. The pH was adjusted using hydrochloric acid and cultures were grown at 180 rpm on a rotary shaker at 30 °C. Selection was done by adding 50 µg/µL Km, 60 µg/µL Cef, and 60 µg/µL FC where appropriate. Table 1 lists the strains used in this study; Table 2 lists the plasmids used in this study.

DNA manipulations

Molecular biology manipulations were done according to standard procedures (Sambrook et al. 1989). For preparation of plasmids, Axyprep Plasmid Miniprep Kit from Axygen (Union City, USA) was used, genomic DNA from *G. oxydans* DSM 3504 and ATCC 621H was extracted with the MasterPure DNA Purification Kit from Epicentre (Madison, USA), and purification of PCR products was done with PCR Clean-up System from Promega (Madison, USA). Restriction enzymes, DNA-ligase, and FastAP (alkaline phosphatase) were purchased from Thermo Fisher Scientific (Waltham, USA). Polymerase chain reaction (PCR) was performed according to the manuals of the supplier Finnzyme (Vantaa, Finland). Phire polymerase was used for analytical tests and Phusion polymerase for amplifications that required proofreading. Oligonucleotides and sequencing were done by Eurofins MWG GmbH (Ebersberg, Germany). Fusion PCR to construct the insert for the deletion vector was carried out according to a long flanking homology (LFH) protocol (Kostner et al. 2013; Wach 1996). Colony PCR was used to screen for correct clones or to confirm the integration of a deletion vector into the genome. The colonies were picked with a pipet tip or toothpick and dissolved in water. The initial 98 °C denaturation step was prolonged to 8 min. Southern blot analysis was done using 1 µg of genomic DNA digested with the appropriate restriction enzyme blotted to a nylon membrane from Roche Diagnostics (Mannheim, Germany). The hybridization was performed overnight with a biotin-labeled 700-bp probe. The Biotin Decalabel and Biotin Chromogenic detection kit from Thermo Fisher Scientific (Waltham, USA) were used for labeling the probe and detection of signals.

Transformation of *Gluconobacter*

Plasmids were transformed in *G. oxydans* DSM 3504 via electroporation (Hall et al. 1992; Kallnik et al. 2010; Mostafa et al. 2002). Cells were grown to an OD₆₀₀ of 0.9 in rich EP medium containing 80 g/L mannitol, 15 g/L yeast extract, 2.5 g/L MgSO₄ × 7H₂O, 1.5 g/L CaCl₂, and 0.5 g/L glycerol adjusted to pH 6. The culture was centrifuged at

Table 1 Strains used in this study

Organism/strain	Features	Reference/source
<i>Escherichia coli</i>		
<i>E. coli</i> DH5 α	F ⁻ , <i>endA1</i> , <i>hdsR17</i> (rk-mk-), <i>supE44</i> , <i>thi1</i> , <i>recA1</i> , <i>gyrA</i> (Nal ^r), <i>relA1</i> , D (<i>lacZYAargF</i>), U169, F80 <i>lacZ</i> DM15	Hanahan (1983)
<i>E. coli</i> TOP10 (Invitrogen)	F ⁻ , <i>mcrA</i> Δ (<i>mrr-hsdRMS-mcrBC</i>), ϕ 80 <i>lacZ</i> DM15, Δ <i>lacX74</i> , <i>nupG</i> , <i>recA1</i> , <i>araD139</i> , Δ (<i>ara-leu</i>)7697, <i>galE15</i> , <i>galK16</i> , <i>rpsL</i> (Str ^R), <i>endA1</i> , λ ⁻	Invitrogen
Acetic acid bacteria		
<i>Gluconobacter oxydans</i> 621H (DSM2343)	Wild type, FC ^R , Cef ^R	De Ley et al. (1984); Gillis and De Ley (1980)
<i>G. oxydans</i> DSM 3504	Wild type, FC ^R , Cef ^R	Motizuki et al. (1966)
<i>G. oxydans</i> DSM 3504 Δ <i>ndh</i>	NADH dehydrogenase deletion strain	This work
<i>G. oxydans</i> DSM 3504 Δ <i>tpiA</i>	Triosephosphate Isomerase deletion strain	This work
<i>G. oxydans</i> DSM 3504 Δ <i>ndh</i> Δ <i>tpiA</i>	NADH dehydrogenase+triosephosphate isomerase deletion strain	This work
<i>G. oxydans</i> DSM 3504 Δ <i>g2dh</i>	Gluconate 2 dehydrogenase deletion strain	This work
<i>G. oxydans</i> 621H Δ 0854 Δ 0855	Polyol dehydrogenase deletion strain, FC ^R , Cef ^R	Kostner et al. unpublished
<i>G. oxydans</i> 621H pAJ78	NADH dehydrogenase overexpression strain	This work

4,000 rpm at 4 °C for 10 min and washed three times in 1 mM HEPES. After distribution of the cells in 50- μ L aliquots, the caps were shock frozen in liquid nitrogen. The electroporation was carried out in cuvettes with 1-mm electrode distance from Peqlab (Erlangen, Germany) with 2.5 kV, 25 μ F, and 400 Ω by a Gene Pulser apparatus from Bio-Rad GmbH (München, Germany). Fresh EP medium was added after the pulse; the cells were incubated on a rotary shaker overnight for a better regeneration and plated out on mannitol plates containing Km.

Transformation of strain ATCC 621H was done by triparental mating. *E. coli* strain TOP10 carrying the vector with mutagenesis insert was used as donor and *E. coli* strain HB101 carrying plasmid pRK2013 as helper strain. *G. oxydans* and *E. coli* cells were grown to an OD₆₀₀ of 0.9, 1 mL of donor and 1 mL of helper strain were mixed and washed with fresh LB, and then 4 mL of *G. oxydans* culture was added and centrifuged. The resulting pellet was resuspended in fresh *G. oxydans* medium and placed on a mannitol containing agar plate in a spot of low coverage. After 24-h

incubation, the cells were washed from the plate with fresh mannitol medium and the resulting cell suspension was plated out on mannitol plates containing Km and Cef.

Construction of the *G. oxydans* deletion strains

The construction of deletion strains of *G. oxydans* DSM 3504 was achieved with the markerless deletion method published by Kostner et al. (2013). In a first step, the two flanking regions comprising approximately 900 bp upstream and downstream of the genes of interest were amplified. Long flanking homology PCR was performed to ligate the products; the two fused fragments were digested with *KpnI* and *XbaI* restriction enzymes and cloned into the dephosphorylated vector pKOS6b. The resulting deletion vector was transformed in *E. coli* TOP10 cells and the insert was verified by colony PCR and sequencing. After transformation of the deletion vector to *G. oxydans*, a homologous recombination event leads to the integration of the vector into the chromosome (first

Table 2 Plasmids used in this study

Plasmid	Features	Reference/source
pKOS6b	Derivative from pAJ63a, <i>upp</i> removed, <i>codBA</i> integrated, Km ^R , FC ^S	This work
pBBR-1 MCS2	Broad-host-range vector, Km ^R	Kovach et al. (1995)
pKOS6b Δ <i>g2dh</i>	Deletion vector based on pKOS6b for deletion of <i>g2dh</i> in <i>G. oxydans</i> DSM 3504, Km ^R , FC ^S	This work
pKOS6b Δ <i>ndh</i>	Deletion vector based on pKOS6b for deletion of <i>ndh</i> in <i>G. oxydans</i> DSM 3504, Km ^R , FC ^S	This work
pKOS6b Δ <i>tpiA</i>	Deletion vector based on pKOS6b for deletion of <i>tpiA</i> in <i>G. oxydans</i> DSM 3504, and <i>G. oxydans</i> DSM3504 Δ 541, Km ^R , FC ^S	This work
pAJ78	Expression vector based on pBBR-1 MCS2 for overexpression of <i>ndh</i> in <i>G. oxydans</i> DSM 3504, Km ^R , FC ^S	This work

recombination). The integration was checked with a genome-specific and a vector-specific primer. The verified clones were plated on mannitol selection plates containing 60 µg/mL FC. A subsequent second recombination caused the replacement of the target gene with the fused gene flanks on the deletion vector in half of the cases. Correct mutants were identified by colony PCR. Sequencing and Southern blotting with a probe targeting the flanking region of the deleted gene verified the in-frame deletion. All the utilized primers are listed in Table 3.

Expression of NADH dehydrogenase

To express the NADH dehydrogenase (NDH-2) from strain DSM 3504 in strain ATCC 621H, a 1.5-kb fragment including the putative promoter region of NDH-2 was amplified with primers *ndhXbaI* fwd and *ndhHindIII* rev (Table 3) using genomic DNA as template. The resulting fragment was digested with *XbaI* and *HindIII*, ligated in the vector pBBR1MCS2 (Kovach et al. 1995), and digested with the same enzymes. After transformation of the resulting vector pAJ78 in *E. coli* DH5α, the insertion was verified by colony PCR and was sequenced using primers pK18MCS_F and pK18MCS_R (Table 3). The vector pBBR1MCS2 carries a Km resistance

cassette, has a copy number of 26±6 (Kallnik et al. 2010), and was therefore chosen for the expression.

Whole-genome sequencing and annotation of *G. oxydans* DSM 3504

The genomic DNA of *G. oxydans* 3504 was isolated using the MasterPure™ DNA purification kit (Epicentre, Madison, WI, USA). The 454-shotgun library was constructed following the GS Rapid library protocol (Roche 454, Branford, USA) and sequenced using the Titanium sequencing kit and the Genome Sequencer FLX (Roche 454). In total, 259,066 reads with 103,263,569 bases were generated resulting in a coverage of 36. The de novo sequence assembly was conducted using Roche Newbler assembly software 2.4 (Roche 454), and the remaining 21 gaps were closed by PCR-based techniques and subsequent Sanger sequencing of the PCR products using BigDye 3.1 chemistry and an ABI3730XL capillary sequencer (Applied Biosystems, Darmstadt). The closed DNA sequence was polished by additional Sanger sequencing to a minimal quality score of Phred 45 employing the Gap4 software of the Staden package (Staden et al. 2000).

Table 3 Primers used in this study

Name	Sequence	Application
0478_Kpn_F	CATGGTACCTGATGAGGCTGCAAGGAG	Amplification of upstream sequence of <i>g2dh</i>
0478_Fus_R	TTTGTCATTGGAGCAAGAAAGTACGGTTTGTTCACCCG	
0478_Fus_F	CGGGTGAACAAACCGTACTTTCTTGCTCCAATGACAAACA	Amplification of downstream sequence of <i>g2dh</i>
0478_XbaI_R	CATAGATCTAGATCGGAGAGGTTCTCCAG	
0478_Check_F	CCTGTGCAGAGGCGTCTC	Confirmation of <i>g2dh</i> Deletion
0478_Check_R2	CATTGTAGCAGACAACGGC	
0541_F_Kpn_up	CATGGTACCTCAGGTCTGCGTTTTCCG	Amplification of upstream sequence of <i>ndh</i>
0541_R_upFUS	TGCTCAGGCGCGGATGGTGCCGGTTTTCCAGGCCTCCG	
0541_F_doFUS	CTTGCTCCGGATTTTGCGCACCATCCGCGCCTGAG	Amplification of downstream sequence of <i>ndh</i>
0541_R_xbaDO	GACTCTAGAGCTGTGTTCCGGCATGA	
0541_check_F	ATGATGCGGACGTCGAAAAG	Confirmation of <i>ndh</i> Deletion
0541_check_R	TCGGGCATTACTGGAATGTG	
sonde_0541nF	GATCTGCATGGACTGATCCG	Amplification of <i>ndh</i> probe for Southern Blot
sonde_0541nR	GCAGGACAGCCATGTCAG	
<i>ndhHindIII</i> rev	ATAAAGCTTTTCAGTCCAGCCGCACGGAAG	Amplification of <i>ndh</i> for overexpression
<i>ndhXbaI</i> fwd	ATATCTAGACGCTCTTTATTACAGTCACC	
0548_Kpn_F	TGAGGTACCGGAAGTCTCGGTACATTCTG	Amplification of upstream sequence of <i>tpiA</i>
0548_FUS_R	GAAACCCTGTCTGTGAGGTTAATGAATGCCGTGCTCGTG	
0548_FUS_F	CACGAGCACGGCATTATTAACCTCACGACAGGGTTTC	Amplification of downstream sequence of <i>tpiA</i>
0548_xba_R	ACGTCTAGACGATGCAGCAGCTCTGT	
0548_check_F	CAACGCTTGAGGACCAGAC	Confirmation of <i>tpiA</i> Deletion
0548_check_R	CCCTCGATGACGAAAAGCG	
0548_sonde_F	CAGCATTGCGGCGTAAG	Amplification of <i>tpiA</i> probe for Southern Blot
0548_sonde_R	TTGACTATGTCACGGAGCG	
pK18MCS_F	TTCCGGCTCGTATGTTGTG	pKOS6b screening primers
pk18MCS_R	GGGCCTCTTCGCTATTACG	
pk18MCS_2R	CAGCTGGCAATTCCGGTTC	

Open reading frame (ORF) prediction was conducted by mapping of *G. oxydans* 621H ORFs to the polished sequence of *G. oxydans* DSM 3504 and additional ORF finding using GLIMMER (Delcher et al. 1999). Subsequently, the predicted ORFs were manually curated based on GC content, GC frame plot, and ribosomal binding sites using Artemis v11.0 (Rutherford et al. 2000). The tools tRNA scan SE (Lowe and Eddy 1997) and RNAmmer (Lagesen et al. 2007) were used for prediction of tRNAs and rRNAs, respectively. The annotation was partially mapped from *G. oxydans* 621H. The remaining ORFs were annotated using the software tool ERGO (Overbeek et al. 2003). The IMG/ER system (Markowitz et al. 2009) was used for additional manual revision of the genome annotation. The annotated sequence of *G. oxydans* DSM3504 was deposited in GeneBank under the accession number CP004373.

Monitoring growth with RAMOS, BioLector, and HPLC

The cultivations were performed using a Respiration Activity Monitoring System (RAMOS) and BioLector with parallel shake flasks for off-line sampling. RAMOS (Anderlei et al. 2004) enables online measurement of oxygen transfer rate (OTR), carbon dioxide transfer rate (CTR), and respiration quotient (RQ) in eight parallel flasks, commercially available from Kuhner (Birsfelden, Switzerland) or Hitech Zang (Herzogenrath, Germany). The CTR indicates the rate of CO₂ formation and the OTR the rate of O₂ consumption of the cells. The integral OTR is a value for the total amount of consumed O₂ during the cultivation. For the off-line sampling, parallel cultivations were performed in 250-mL unbaffled shake flasks at identical conditions as the RAMOS cultivations (30 °C, 50-mm shaking diameter) in an ISF-4-W Kuhner shaker (Birsfelden, Switzerland). Each sample flask was used only once for sampling to avoid a change in culture volume. *G. oxydans* was inoculated from a glycerol stock; for a better growth, the preculture was cultivated in a medium containing 440 mM (8 % w/v) mannitol, 4 g/L yeast extract, 2.5 g/L MgSO₄ × 7 H₂O, 1 g/L (NH₄)₂SO₄, and 1 g/L KH₂PO₄ at pH 6 overnight at 30 °C. Cef was added to the preculture to prevent contaminations. The main culture was inoculated to an initial OD₆₀₀ of 0.1 with 10-mL filling volume and grown at 30 °C with a shaking frequency of 300 rpm in mannitol standard medium as described in the cultivation section. Km was added to the cultures of strains carrying the NDH-2 expression vector to ensure selective pressure. Several samples were taken at selected time points and analyzed regarding pH, optical density, and sugar concentrations. BioLector enables online measurements of biomass by observing light scattered by the cells and fluorescent metabolites such as NADH and FAD that are representative for cell constituents. In addition, it allows online monitoring of pH in parallel fermentations in microtiter plates (Huber et al. 2010; Kensy

et al. 2009). The experimental conditions were 995 rpm shake frequency, 3-mm shaking diameter, and 1-mL filling volume in a Flower Plate from m2p-Labs (Aachen, Germany). For the analysis of the off-line samples with HPLC, 1-mL culture was centrifuged for 5 min at 10,000×g and the supernatant was filtered through a 0.2-μm PVDF filter from Carl Roth (Karlsruhe, Germany). The experiments were performed with HPLC System 10A Series from Shimadzu (Kyoto, Japan) with a carbohydrate Pb²⁺ column (300×8) including a pre-column from CS-Chromatographie Service (Langerwehe, Germany) at 80 °C with H₂O as eluent and a flow rate of 0.6 mL/min. The retention times for fructose and mannitol were 20 and 30 min, respectively.

Results

Whole-genome sequencing of *G. oxydans* DSM 3504 and comparison to ATCC 621H

G. oxydans DSM 3504 shows nearly a threefold higher growth yield than strain ATCC 621H on glucose (Elfari et al. 2005). In order to determine whether there is an identifiable genomic reason for this high discrepancy in growth, we sequenced the genome of strain DSM 3504. The genome comparison between DSM 3504 and ATCC 621H using ERGO and a protein-sequence-based bidirectional BLAST approach revealed that both strains have a similar GC content of 61.03 and 60.82 %, respectively. Plasmids were not detected in DSM 3504 but in ATCC 621H, which harbors five plasmids ranging from 2.6 to 163 kb (Prust et al. 2005). DSM 3504 contains a total of 2,465 ORFs, which is slightly less than the 2,668 ORFs encoded by the genome of ATCC 621H. The main characteristics of the metabolism encoded by both *Gluconobacter* genomes were highly similar. Both strains lack a phosphofructokinase-encoding gene and, therefore, a complete glycolysis is absent, whereas genes for an Entner-Doudoroff pathway and an operon coding for an oxidative pentose phosphate cycle are present. Common is also the absence of a complete tricarboxylic acid cycle due to a missing succinate dehydrogenase, which is unusual for aerobic organisms. Genes of central metabolism generally share a high amino acid sequence homology ranging from 93 to 99.7 % between both *Gluconobacter* strains.

A total of 345 ORFs were identified exclusively in DSM 3504; the vast majority encode hypothetical proteins (data not shown). Therefore, we focused the comparison specifically on differing functionally annotated genes with potential relevance on the growth behavior of DSM 3504. Most prominent is GLS_c05650 (NDH-2) coding for an additional type II NADH dehydrogenase (*ndh*) with an identity of 43 % to the sole NADH dehydrogenase of ATCC 621H. Furthermore,

DSM 3504 contains a gene for an extra triosephosphate isomerase (TPI) GLS_c05720 (*tpiA*), which is present in addition to two TPIs that were also found in ATCC 621H. Both exhibited high amino acid sequence homologies of 96.7 and 99.6 % to their counterparts in the other strain. In contrast, the additional TPI only has an amino acid similarity of 68.4 % to the most similar TPI (GOX0900) of ATCC 621H. Two further genes included in our analysis are genes GLS_c05030 and GLS_c05040 coding for two subunits of an extra gluconate 2-dehydrogenase (subsequently called *g2dh* gene) in DSM 3504, which is present in addition to the gluconate 2-dehydrogenase of ATCC 621H.

Construction of DSM 3504 deletion strains and expression of the additional NADH dehydrogenase in ATCC 621H

To test the influence of the selected genes on the growth behavior of DSM 3504, markerless deletion strains of *ndh*, *tpiA*, *g2dh*, and a double mutant *ndh/tpiA* were constructed. The successful deletion of the genes and the absence of the deletion vector from the chromosome were checked by colony PCR and Southern blot analysis (data not shown).

Furthermore, an expression vector was constructed and transformed in strain ATCC 621H to examine the influence of the additional NADH dehydrogenase (*ndh*) from DSM 3504 on the growth of ATCC 621H.

Growth of DSM 3504 Δndh

In order to test whether the additional NDH-2 has significant influence on growth, we compared the growth and NADH and FAD content of the Δndh mutant of DSM3504 to the wild type (wt) with BioLector. Mannitol was used as the carbon source for the cultivation. In comparison to the wt, the Δndh strain showed a significantly slower growth. After 30 h of growth, the resulting biomass of the Δndh strain was more than 30 % less than the wt strain. Also, the final NADH concentration is 45 % and the FAD concentration 30 % lower in the mutant (Fig. 1c, f).

NADH dehydrogenases channel electrons from NADH to the respiratory chain. In order to monitor the respiratory activity in greater detail, we measured the oxygen (OTR) and carbon dioxide transfer rates (CTR) using RAMOS. All those values were significantly lower in the Δndh mutant than in the wt, meaning that the mutant transfers electrons less efficiently to oxygen and produces less carbon dioxide. The OTR and CTR values are sharply increasing in the wt during the first 11 h of growth and then reach a maximum level of about 30 mmol/L/h (Fig. 1b). In the Δndh mutant, the increase of OTR and CTR showed a first peak after 6 h and a second peak after 11 h of growth, with a maximum value of only 11 mmol/L/h (Fig. 1e). After their peak at 11 h of growth, the OTR and CTR are decreasing sharply in both strains. The

integral OTR represents the cumulative amount of consumed oxygen until a specific time point. Again, it can be seen that the mutant consumes significantly less oxygen (140 mmol/L) than the wt (200 mmol/L) strains (Fig. 1b, e). The above online measurements were completed by the off-line determination of OD₆₀₀, pH, and mannitol and fructose concentration at four different time points during the culture (Fig. 1a, d). The mannitol as well as the fructose concentration was determined by HPLC in order to measure substrate consumption. The course of pH values for both strains revealed no difference during the whole cultivation period (Fig. 1a, d). The OD₆₀₀ showed no significant differences during the first 5 h. After 7 h, the OD₆₀₀ was slightly higher in the wt, and after 24 h, there was a distinctive difference of the OD₆₀₀ in the wt (4.9) and the Δndh mutant (3.8) (Fig. 1a, d). This data corresponds well to the scattered light online data from the BioLector. Mannitol is completely consumed after 7 h while the fructose level is increasing due to the conversion of mannitol to fructose. After an initial phase of fructose production, the cells are consuming the produced fructose. The major difference visible between the wt and the Δndh strain is the remaining amount of fructose in the medium. In the wt, approximately 1.5 g/L fructose remained in the medium while this value is 2.9 g/L for the mutant. The numerical data of Fig. 1 can be found in Supplementary Tables S1, S2, and S7.

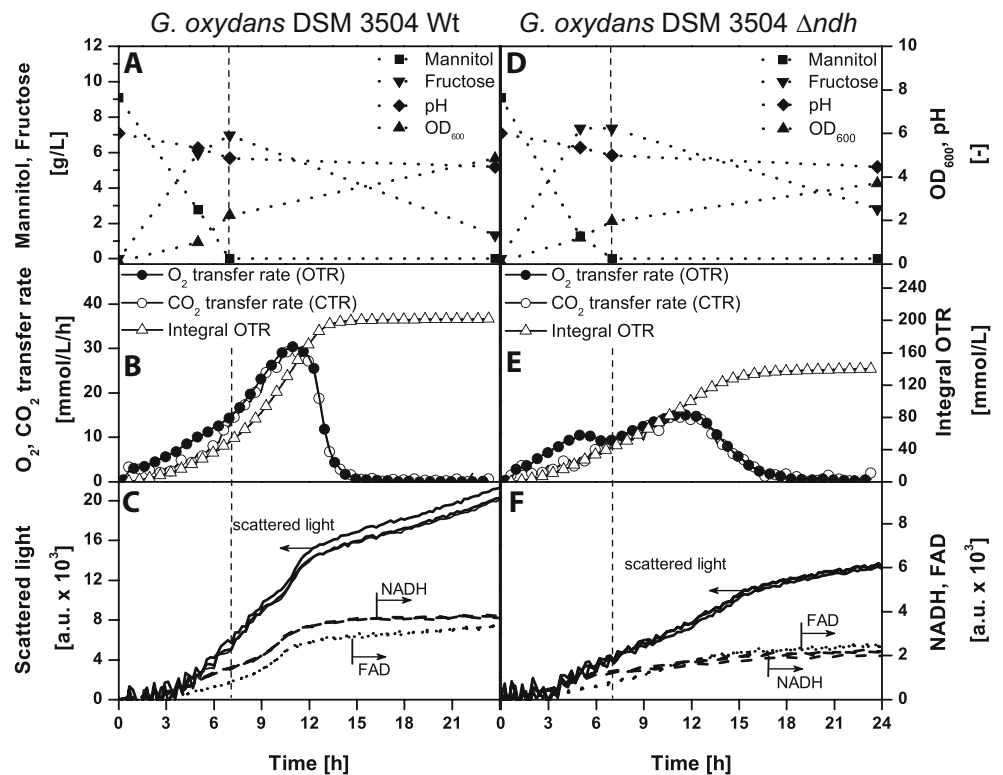
Growth of DSM 3504 $\Delta tpiA$

Another gene, which we assumed to have potential effects on cell growth, is the gene coding for the additional triosephosphate isomerase in DSM 3504. Indeed, the scattered light as well as the NADH and FAD concentrations measured by BioLector showed a weaker growth and a decrease of the NADH and FAD levels of the $\Delta tpiA$ mutant as compared to the wt throughout the cultivation with a slight increase of the growth rate after 13 h (Figs. 1c and 2c). The analysis of OTR and CTR data as determined by RAMOS also showed lower transfer rates matching the weaker growth of the $\Delta tpiA$ strain. The mutant reached maximum values of about 24 mmol/L/h compared to 30 mmol/L/h of the wt. Also, the integrated OTR reached decreases from 200 mmol/L in wt to 180 mmol/L (Figs. 1b and 2b). The course of pH values for both strains again revealed no difference during the whole cultivation period, but the OD₆₀₀ in accordance to the scattered light data revealed a lower growth. After 24 h of cultivation, the OD₆₀₀ of the mutant remains below 4, compared to the wt that reached an OD₆₀₀ of 4.9 (Figs. 1a and 2a). The numerical data of Fig. 2 can be found in Supplementary Tables S3, S4, and S7.

Growth of DSM 3504 $\Delta ndh \Delta tpiA$

As we showed above, the *ndh* as well as the *tpiA* gene has influence on the growth of *G. oxydans* DSM 3504. In a next

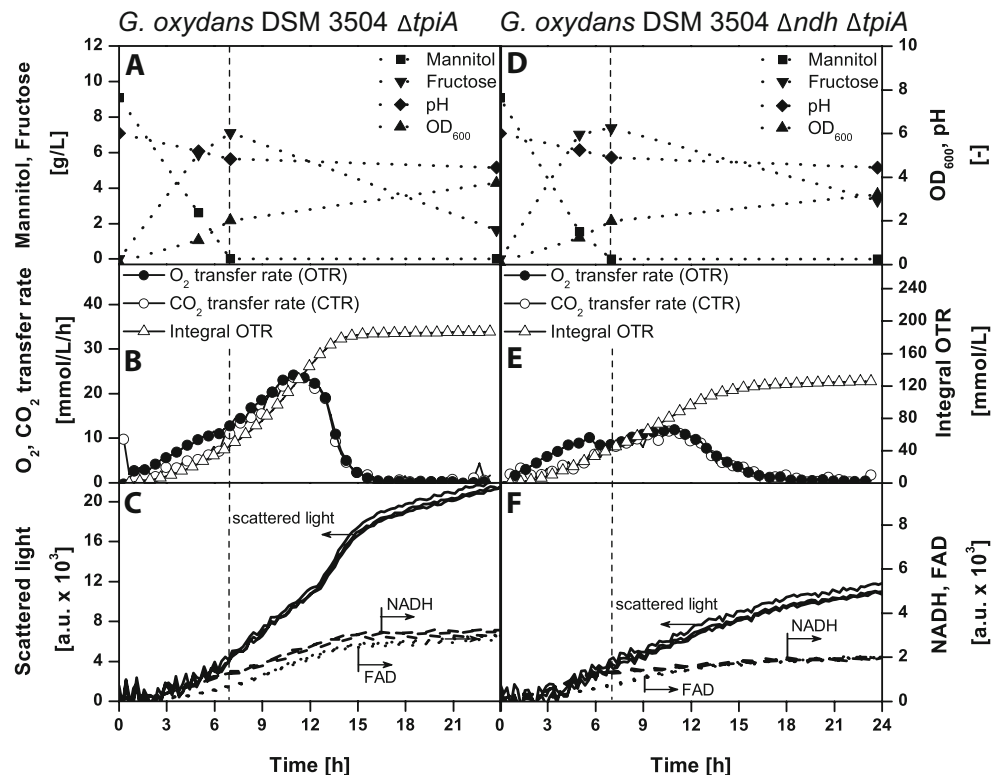
Fig. 1 Data from growth analysis of *G. oxydans* DSM 3504 wt and DSM 3504 Δndh . **a, d** Substrate consumption rates, pH value, and OD₆₀₀; **b, e** RAMOS data with OTR (oxygen transfer rates), CTR (carbon dioxide transfer rates), and integral OTR values (for a better illustration, not every data point is represented by a symbol); **c, f** growth curve measured by scattered light and NADH/FAD progression data from BioLector



step, we wanted to study the consequences of a combination of Δndh and $\Delta tpiA$ genes on the growth of this strain. Therefore, we constructed a double deletion strain *G. oxydans*

DSM 3504 $\Delta 0541\Delta 0548$. The BioLector data of a culture of this strain growing on mannitol showed a further decline of the scattered light curve in comparison to the DSM 3504 Δndh

Fig. 2 Data from growth analysis of *G. oxydans* DSM 3504 $\Delta tpiA$ and DSM 3504 $\Delta ndh \Delta tpiA$. **a, d** Substrate consumption rates, pH value, and OD₆₀₀; **b, e** RAMOS data with OTR (oxygen transfer rates), CTR (carbon dioxide transfer rates), and integral OTR values (for a better illustration, not every data point is represented by a symbol); **c, f** growth curve measured by scattered light and NADH/FAD progression data from BioLector



single mutant. Also, the NADH and FAD levels were significantly lower when compared to the wt and the $\Delta tpiA$ mutant and slightly lower than in the Δndh single mutant (Figs. 1c, f and 2c, f). The evaluation of the RAMOS data confirmed this tendency: Compared to the Δndh strain, the OTR and CTR decreased and the integral OTR declined from 140 mmol/L in the Δndh strain and 180 mmol/L in the $\Delta tpiA$ strain to 120 mmol/L (Figs. 1e and 2b, e). The pH levels and the mannitol consumption graphs showed no difference when compared to the other strains, but the final fructose concentration in the medium was 3.4 g/L and therefore the highest of all tested strains. In accordance to the scattered light values, the OD₆₀₀ values were lower than with the Δndh strain (Figs. 1d and 2d). Consequently, the produced biomass in the $\Delta ndh\Delta tpiA$ double deletion strain is the lowest in comparison to the other strains.

Growth of DSM 3504 $\Delta g2dh$

In contrast to the Δndh , the $\Delta tpiA$, and the $\Delta ndh\Delta tpiA$ strains, the data from BioLector and from RAMOS showed no significant differences between the $\Delta g2dh$ strain and the wt (data not shown). Consequently, there is no influence of the gluconate-2-dehydrogenase on the growth on mannitol.

Expression of the additional NDH-2 from DSM 3504 in strain ATCC 621H

After we observed the decrease of growth of strain DSM 3504 when one of its two *ndh* genes is deleted, we wanted to investigate how strain ATCC 621H behaves, when we introduce the gene for the additional NDH-2 on a plasmid. Already during the precultures, the increased growth of strain ATCC 621H with the second NDH-2 from strain DSM 3504 expressed from its own promoter on plasmid pAJ78 was remarkable. Monitoring the growth with BioLector supported this observation and revealed a huge increase in all measured parameters when the plasmid is present. The scattered light enlarged from a maximal value of 6×10^3 a.u. in the wt to 40×10^3 a.u. in the pAJ78 containing strain. The FAD concentration reached rose from 1×10^3 to 23×10^3 a.u. and NADH from 1×10^3 to 40×10^3 a.u. (Fig. 3c, f). The data from RAMOS also showed a strong effect of the additional copies of NADH dehydrogenase in ATCC 621H. OTR and CTR increased remarkably; the total oxygen consumption measured by the integral OTR rose from 78 mmol/L in the wt to 130 mmol/L in the pAJ78 containing strain (Fig. 3b, e). HPLC analysis of off-line samples revealed for the pAJ78 containing strain a steady, slow decline of the mannitol concentrations in the medium and a nearly undetectable quantity of fructose throughout the culture. In accordance to the BioLector data, the OD₆₀₀ reached was boosted from 1.8 for the wt to a level of 4 for the pAJ78 containing strain. Each of the above data

confirmed the strong and profound influence of the NADH dehydrogenase on the growth behavior and biomass formation of *G. oxydans*. The numerical data of Fig. 3 can be found in Supplementary Tables S5, S6, and S7.

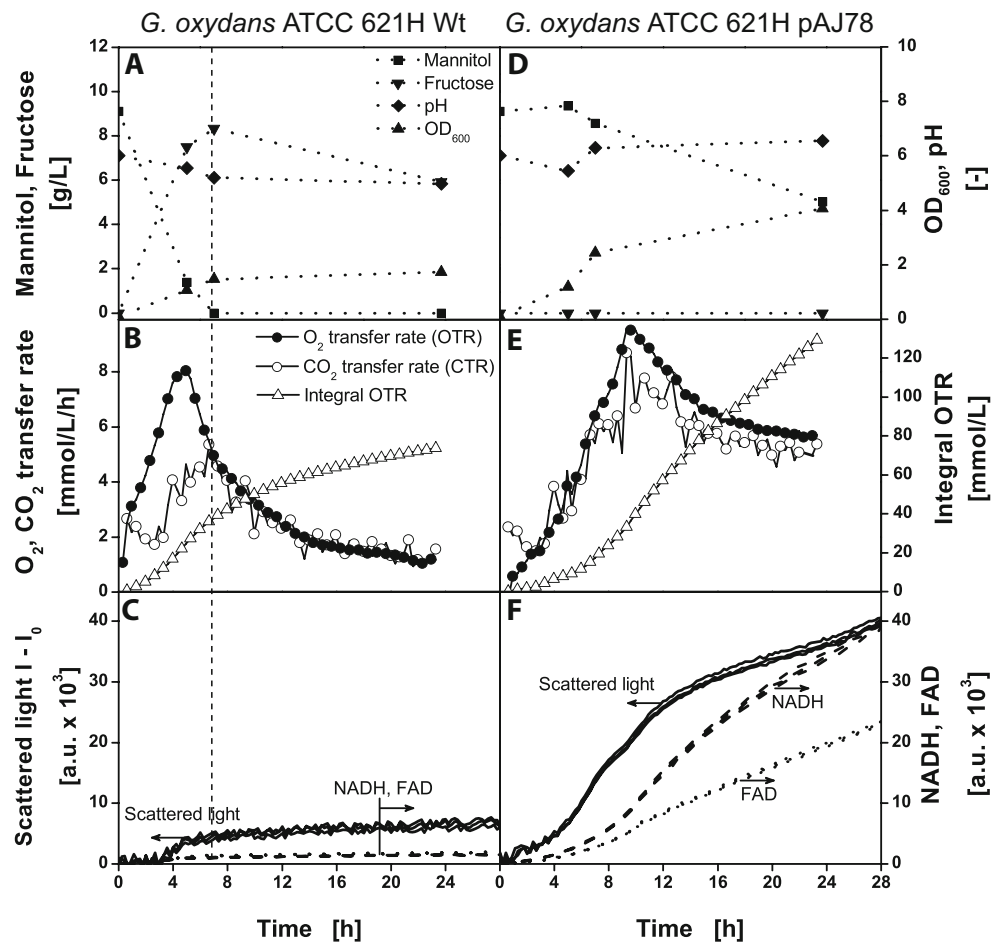
Discussion

In this study, we have shown that despite of the significant differences in the growth yields, the genome sequences and the central metabolic pathways of the *G. oxydans* strains DSM 3504 and ATCC 621H are very similar. The comparison of sequence data revealed 345 ORFs that are exclusively present in DSM 3504, but most of them are hypothetical. In search of an explanation of the differing growth behavior of the two *G. oxydans* strains, we focused on the three differed annotated genes that are potentially part of the central metabolism. GLS_c05650 (*ndh*) encodes an additional class II NADH dehydrogenase that catalyzes the transfer of electrons from NADH to ubiquinone (Friedrich and Scheide 2000; Jaworowski et al. 1981) and thereby supplies electrons to the respiratory chain (Cava et al. 2004). For that reason, it seemed auspicious to examine this gene particularly. The *tpiA* gene codes for a glycolytic triosephosphate isomerase (TPI) that catalyzes the reversible conversion from dihydroxyacetone-phosphate (DHAP) to glyceraldehyde-3-phosphate (GAP) (Knowles 1991) This gene is present in an additional copy in DSM 3504 beside the two paralogs present in ATCC 621H. Given the fact that the TPI is considered to be a very active enzyme (Rose et al. 1990), it seemed peculiar that strain DSM 3504 contains a third copy of this gene. A possible explanation could be differential regulation of the paralogs. The third candidate we have chosen to test the potential influence on the growth performance was a soluble gluconate 2-dehydrogenase (G2dh) that catalyzes the conversion of D-gluconate to 2-keto-D-gluconate with high specificity (Levering et al. 1988; Matsushita et al. 1982). Strain DSM 3504 again contains an additional paralog of a G2dh, which is lacking in ATCC 621H.

While we have not observed a phenotype for the *g2dh* mutation in DSM 3504 during growth on mannitol, the deletion of the genes for the additional copies of *ndh* and *tpiA* from DSM 3504 each showed a distinct influence on the phenotype in our growth analyses. The growth of the Δndh strain was most profoundly affected.

To understand the presented data, it is important to notice that the membrane-bound polyol dehydrogenase (Polyol DH) catalyzes the oxidation of mannitol to fructose outside of the cell (Peters et al. 2013b; Voss et al. 2010). The electrons from this oxidation are fed via ubiquinone in the short electron transport chain and are finally reducing oxygen (Fig. 4) (Matsushita et al. 1994). No CO₂ is formed during this oxidation. Therefore, mannitol oxidation by Polyol DH leads to O₂

Fig. 3 Comparison of data from growth analysis of *G. oxydans* ATCC 621H wt and NADH dehydrogenase overexpression strain. **a, d** Substrate consumption rates, pH value, and OD₆₀₀; **b, e** RAMOS data with OTR, CTR, and integral OTR values (for a better illustration, not every data point is represented by a symbol); **c, f** Growth curve measured by scattered light and NADH/FAD progression data from BioLector



consumption but no CO₂ formation. *G. oxydans* cannot assimilate mannitol directly, but the formed fructose is taken up

(Peters et al. 2013a, b) and oxidized to acetate as an end product via the pentose-phosphate pathway (PPP) and a

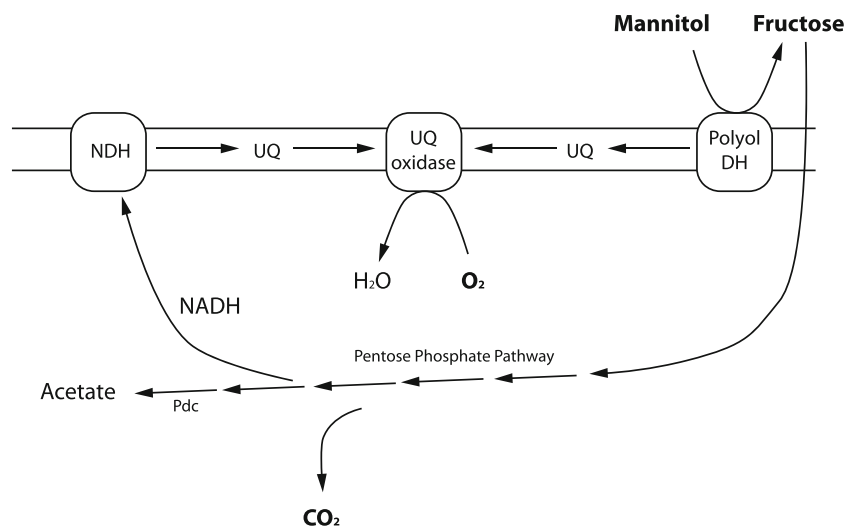


Fig. 4 Overview on growth on mannitol by *G. oxydans*. Mannitol is oxidized to fructose outside of the cell by membrane-bound polyol dehydrogenase (Polyol DH). Electrons from this oxidation are directly fed in the electron transport chain. The fructose is then assimilated and oxidized, accompanied by CO₂ formation, via the pentose-phosphate

pathway (PPP) and pyruvate-decarboxylase (Pdc) to acetate. The redox equivalents are transferred via NADH and the NAD dehydrogenase (NDH) to the electron transport chain finally reducing O₂ via UQ oxidase (UQ ubiquinone)

pyruvate decarboxylase reaction (Fig. 4) (Peters et al. 2013a, b; Richhardt et al. 2012). During the oxidation of fructose to acetate, CO₂ is formed and redox equivalents are transferred via NADH and the NDH to the electron transport chain finally reducing O₂. Therefore, fructose oxidation by soluble metabolism leads to O₂ consumption together with CO₂ formation. Soluble metabolism results in cell mass formation by using part of the assimilated carbon compounds for biosynthesis, while substrate oxidation by membrane-bound dehydrogenases does not result in cell mass formation because only electrons flow through the respiratory chain, but no carbon is assimilated. In Figs. 1, 2, and 3, the dashed vertical line marks the point of time, when mannitol is depleted and therefore no more substrate oxidation by the Polyol DH can occur. Afterwards, only fructose can be metabolized and used for the formation of cell mass, although a minor part of the fructose is lost by formation of 5-ketofructose. The period of mannitol or fructose utilization in the cultures is subsequently called phase I and phase II.

As can be seen in Fig. 1b, the consumption of O₂ in DSM 3504 wt increases together with the cell mass. The OTR (closed circles) value during phase I is higher than the CTR (open circles) value and increases further during period II. When mannitol is depleted, marked by the dashed line, the difference between the OTR and CTR values disappears. This indicates that in period II, the electrons are channeled in the electron transport chain via NADH. The high CO₂ formation reflects the strong formation of biomass, which can be observed in the scattered light data. After 13 h, much of the fructose is consumed and O₂ and CO₂ consumption drops to zero. Therefore, the flow of electrons through the respiratory chain decreases substantially, the rise of biomass as measured by scattered light slows down, and cell components (NADH / FAD) are no longer increasing. The slight increase of scattered light values is eventually due to the altered cell morphology. These results indicate that the oxidation of the substrate fructose by the soluble metabolism is active in both phases, but the activity is rising considerably during phase II. High amounts of NADH are channeled to the respiratory chain via the two NDH. This hints to the important role of NDH for biomass formation in *G. oxydans*.

Strain ATCC 621H produces considerably less biomass than DSM 3504 (Fig. 3a, c). During phase I, the O₂ consumption is significantly higher than the CO₂ production, which reveals that the membrane bound polyol DH is very active. The flow of electrons is only moderately increasing during phase II (integral OTR), but the OTR and CTR are decreasing significantly and there is no difference between the two rates. This indicates that the membrane-bound polyol DH channels the main share of electrons in the respiratory chain from oxidation of mannitol and much less electrons are coming from fructose breakdown in the cytoplasm and the NDH. Accordingly, fructose is metabolized very slowly, and after

the flattening of the growth curve, the level of remaining unutilized fructose is high. The strain is not able to utilize fructose efficiently and the biomass yield is low, because biomass is formed by carbon assimilation through the soluble metabolism. This corresponds well to the view of Prust et al. (2005), postulating that the low biomass yield of strain ATCC 621H is due to the very active membrane bound dehydrogenases in this strain.

In DSM 3504 Δndh , the difference between O₂ consumption (OTR) and CO₂ formation (CTR) during phase I is higher than in the wt showing a distinct peak somehow resembling the situation in strain ATCC 621H (Fig. 1d, e, f) although the growth is still higher in the Δndh strain. Due to the deletion of one NDH, there is a higher flow of electrons through the membrane-bound polyol DH into the electron transport chain. The polyol DH and the NDH seem to compete for feeding electrons in the respiratory chain. Therefore, the activity of the polyol DH is higher than substrate oxidation by cytoplasmic enzymes, due to the loss of one NDH. In phase II, the difference between OTR and CTR disappears, because the mannitol is consumed and fructose is assimilated, but growth is significantly lower than in the wt. The Δndh strain is metabolizing fructose less efficiently through its cytoplasmic enzyme systems due to the loss of one NDH presumably because NADH is oxidized more slowly than in the wt. As long as mannitol is available, the competing polyol DH is more active. This is a similar situation as in ATCC 621H with his high active membrane-bound dehydrogenases and only one NDH. The presence of a second NDH in *G. oxydans* facilitates the competition with membrane-bound dehydrogenases and enables an efficient reoxidation of NADH.

Confirmation of this view on the growth physiology of *G. oxydans* was obtained by overexpression of NDH from plasmid pAJ78 (Fig. 3d, e, f). Right from the beginning, there was no difference between O₂ consumption and CO₂ formation. The values, including biomass formation, are decidedly higher than in the wt. The higher flow of electrons through the transport chain (integral OTR) is probably due to a faster transfer of electrons from NADH into the respiratory chain. The formation of cell components as measured by NADH, FAD, and biomass increases sharply. The assimilation of fructose occurs with a high rate, because in contrast to all other examined strains, an intermediate accumulation of the sugar in the medium is not measurable. The limiting activity in the NDH overexpression strain seems to be the polyol DH forming fructose from mannitol, probably because the enzyme is not able to transfer the electrons into the respiratory chain, due to competition with NDH. Accordingly, the mannitol is never completely consumed during the experiment. The more electrons are channeled in the respiratory chain via NADH, the less activity the polyol DH has. This experiment shows that increased NDH activity is beneficial for the formation of biomass.

The influence of the additional TPI isoenzyme found in DSM 3504 on growth is smaller than that of the NDH but also significant. Growth of the DSM 3504 $\Delta tpiA$ mutant was weaker than in the wt, and OTR, CTR, and biomass values reached were lower than in wt (Fig. 2a, b, c). This reduced growth performance hints to a bottleneck in the carbon flux through the central metabolism at the TPI. Regarding the high efficiency of TPI, the exact reason of this shortage remains unknown but could be attributed either to the regulation of the isoenzymes or differing substrate specificity.

The double deletion strain $\Delta ndh \Delta tpiA$ was created to examine the combined effects of the individual mutations with influence on growth of *G. oxydans* in a single strain. All measured growth parameters exhibit a slight decrease in comparison to the Δndh strain (Figs. 1d, e, f and 2d, e, f). This shows a clear combined effect of the *ndh* and *tpiA* deletion compared to the wt and the single deletion strains. Nevertheless, the influence of the $\Delta tpiA$ mutation on the production of biomass proves again to be much smaller than that of the Δndh . Overexpression of TPI from DSM 3504 in ATCC 621H resulted in no measurable increase of the produced biomass (data not shown).

In this study, we were able to identify two enzymes that influence the growth characteristics of *G. oxydans* considerably. Most profoundly, the introduction of plasmid pAJ78 with an additional copy of a *ndh* gene from DSM 3504 in ATCC 621H resulted in a remarkable raise of growth accompanied by a sharp decrease of the activity of membrane-bound polyol dehydrogenase. These results reflect the special physiological aspects of acetic acid bacteria. In contrast, a study with *Corynebacterium glutamicum* showed that the overexpression of NADH dehydrogenases had negative effects on growth (Nantapong et al. 2004). In acetic acid bacteria, the membrane-bound dehydrogenases seem to compete with the NDH for channeling electrons in the respiration chain. Confirming these conclusions, the deletion of one *ndh* copy from DSM 3504 led to a considerably decline of growth and to an increase of the activity of the membrane-bound polyol dehydrogenase. These insights should be very useful for the optimization of *Gluconobacter* strains for biotechnological oxidative fermentations. The industrial application of the strains is often restricted by a poor biomass yield. On the other hand, production strains are required to have a high activity of their membrane-bound dehydrogenases. This study suggests that the activity of the NADH dehydrogenase is a key factor controlling activity of membrane-bound dehydrogenases and biomass formation. Under natural growth conditions, NADH accumulation might slow down the flux through the soluble metabolism either by allosteric regulations or by equilibrium. Or, most NADH in *Gluconobacter* growing in the habitat is used for assimilation of oxidized substrates by soluble dehydrogenases. It is interesting that recent studies pointed to a growth limitation by cytochrome bo_3 oxidase (Richhardt et al.

2013). When the capacity of the electron transport chain is limiting growth of *G. oxydans* (Meyer et al. 2013), this in turn leads to a high competition between NDH and membrane-bound dehydrogenases for feeding electrons in the saturated electron transport chain. The growth limitation by the electron transport chain could be the reason for the relatively simple structure of the electron transport chain of *Gluconobacter*, lacking a cytochrome *c* oxidase. Due to limited membrane space, the requirement of an additional complex would further limit the capacity of the respiratory chain. Therefore, the evolutionary tendency of the electron transport chain in *Gluconobacter* seems to be simple, but as high capacity as possible. If these factors could be controlled in metabolic engineering approaches, for example by varying the expression or copy number of the NADH dehydrogenase or freeing membrane space by deleting unnecessary membrane-bound dehydrogenases, the biotechnological usefulness of *Gluconobacter* as an oxidative catalyst could be increased considerably. Potentially, these findings are valid not only for the genus *Gluconobacter* but also for many other acetic acid bacteria. Furthermore, the study underscores that whole-genome sequencing can be very helpful to get insights in physiological differences between different strains and emphasizes the high relevance of connecting a genome-sequencing approach with molecular biology and detailed physiologic experiments.

Acknowledgments We thank the Bundesministerium für Bildung und Forschung (BMBF) for funding this work in the framework of the GenoMik-Transfer initiative (FKZ: 0315632C).

References

- Anderlei T, Zang W, Papaspyrou E, Büchs J (2004) Online respiration activity measurement (OTR, CTR, RQ) in shake flasks. *Biochem Eng J* 17:187–194
- Cava F, Zafra O, Magalon A, Blasco F, Berenguer J (2004) A new type of NADH dehydrogenase specific for nitrate respiration in the extreme thermophile *Thermus thermophilus*. *J Biol Chem* 279(44):45369–45378
- De Ley J, Swings J, Gossele F (1984) The genus *Gluconobacter*. In: Krieg N, Holt J (eds) *Bergey's manual of systematic bacteriology*. Williams & Wilkins Co., Baltimore, pp 267–278
- De Muynck C, Pereira CS, Naessens M, Parmentier S, Soetaert W, Vandamme EJ (2007) The genus *Gluconobacter oxydans*: comprehensive overview of biochemistry and biotechnological applications. *Crit Rev Biotechnol* 27(3):147–171
- Delcher AL, Harmon D, Kasif S, White O, Salzberg SL (1999) Improved microbial gene identification with GLIMMER. *Nucleic Acids Res* 27(23):4636–4641
- Deppenmeier U, Ehrenreich A (2009) Physiology of acetic acid bacteria in light of the genome sequence of *Gluconobacter oxydans*. *J Mol Microbiol Biotechnol* 16(1–2):69–80
- Deppenmeier U, Hoffmeister M, Prust C (2002) Biochemistry and biotechnological applications of *Gluconobacter* strains. *Appl Microbiol Biotechnol* 60(3):233–242

- Elfari M, Ha S-W, Bremus C, Merfort M, Khodaverdi V, Herrmann U, Sahn H, Görisch H (2005) A *Gluconobacter oxydans* mutant converting glucose almost quantitatively to 5-keto-D-gluconic acid. *Appl Microbiol Biotechnol* 66(6):668–674
- Friedrich T, Scheide D (2000) The respiratory complex I of bacteria, archaea and eukarya and its module common with membrane-bound multisubunit hydrogenases. *FEBS Lett* 479(1–2):1–5
- Gillis M, De Ley J (1980) Intra- and intergeneric similarities of the ribosomal ribonucleic acid cistrons of *Acetobacter* and *Gluconobacter*. *Int J Sys Bacteriol* 30:7–27
- Gupta A, Singh VK, Qazi GN, Kumar A (2001) *Gluconobacter oxydans*: its biotechnological applications. *J Mol Microbiol Biotechnol* 3(3):445–456
- Hall PE, Anderson SM, Johnston DM, Cannon RE (1992) Transformation of *Acetobacter xylinum* with plasmid DNA by electroporation. *Plasmid* 28(3):194–200
- Hanahan D (1983) Studies on transformation of *Escherichia coli* with plasmids. *J Mol Biol* 166(4):557–580
- Huber R, Palmen TG, Ryk N, Hillmer AK, Luft K, Kesy F, Büchs J (2010) Replication methods and tools in high-throughput cultivation processes—recognizing potential variations of growth and product formation by on-line monitoring. *BMC Biotechnol* 10:22
- Jaworowski A, Campbell HD, Poulis MI, Young IG (1981) Genetic identification and purification of the respiratory NADH dehydrogenase of *Escherichia coli*. *Biochemistry* 20(7):2041–2047
- Kallnik V, Meyer M, Deppenmeier U, Schweiger P (2010) Construction of expression vectors for protein production in *Gluconobacter oxydans*. *J Biotechnol* 150(4):460–465
- Kesy F, Zang E, Faulhammer C, Tan RK, Büchs J (2009) Validation of a high-throughput fermentation system based on online monitoring of biomass and fluorescence in continuously shaken microtiter plates. *Microb Cell Fact* 8:31
- Knowles JR (1991) Enzyme catalysis: not different, just better. *Nature* 350(6314):121–124
- Kostner D, Peters B, Mientus M, Liebl W, Ehrenreich A (2013) Importance of *codB* for new *codA*-based markerless gene deletion in *Gluconobacter* strains. *Appl Microbiol Biotechnol* 97(18):8341–8349
- Kovach ME, Elzer PH, Hill DS, Robertson GT, Farris MA, Roop RM, Peterson KM (1995) Four new derivatives of the broad-host-range cloning vector pBRR1MCS, carrying different antibiotic-resistance cassettes. *Gene* 166(1):175–176
- Lagesen K, Hallin P, Rodland EA, Staerfeldt HH, Rognes T, Ussery DW (2007) RNAmmer: consistent and rapid annotation of ribosomal RNA genes. *Nucleic Acids Res* 35(9):3100–3108
- Levering PR, Weenk G, Olijve W, Dijkhuizen L, Harder W (1988) Regulation of gluconate and ketogluconate production in *Gluconobacter oxydans* ATCC 621-H. *Arch Microbiol* 149:534–539
- Lowe TM, Eddy SR (1997) tRNAscan-SE: a program for improved detection of transfer RNA genes in genomic sequence. *Nucleic Acids Res* 25(5):955–964
- Markowitz VM, Mavromatis K, Ivanova NN, Chen IM, Chu K, Kyrpides NC (2009) IMG ER: a system for microbial genome annotation expert review and curation. *Bioinformatics* 25(17):2271–2278
- Matsushita K, Shinagawa E, Ameyama M (1982) D-Gluconate dehydrogenase from bacteria, 2-keto-D-gluconate-yielding, membrane-bound. *Methods Enzymol* 89 Pt D:187–193
- Matsushita K, Toyama H, Adachi O (1994) Respiratory chains and bioenergetics of acetic acid bacteria. *Adv Microb Physiol* 36:247–301
- Meyer M, Schweiger P, Deppenmeier U (2013) Effects of membrane-bound glucose dehydrogenase overproduction on the respiratory chain of *Gluconobacter oxydans*. *Appl Microbiol Biotechnol* 97(8):3457–3466
- Mostafa HE, Heller KJ, Geis A (2002) Cloning of *Escherichia coli lacZ* and *lacY* genes and their expression in *Gluconobacter oxydans* and *Acetobacter liquefaciens*. *Appl Environ Microbiol* 68(5):2619–2623
- Motizuki K, Takarazuka I, Kanzaki T (1966) Method for producing 2-keto-L-gulonic acid
- Nantapong N, Kugimiya Y, Toyama H, Adachi O, Matsushita K (2004) Effect of NADH dehydrogenase-disruption and over-expression on respiration-related metabolism in *Corynebacterium glutamicum* KY9714. *Appl Microbiol Biotechnol* 66(2):187–193
- Overbeek R, Larsen N, Walunas T, D'Souza M, Pusch G, Selkov E, Liolios G, Joukov V, Kaznadzey D, Anderson I, Bhattacharyya A, Burd H, Gardner W, Hanke P, Kapatral V, Mikhailova N, Vasieva O, Osterman A, Vonstein V, Fonstein M, Ivanova N, Kyrpides N (2003) The ERGO genome analysis and discovery system. *Nucleic Acids Res* 31(1):164–171
- Peters B, Junker A, Brauer K, Mühlthaler B, Kostner D, Mientus M, Liebl W, Ehrenreich A (2013a) Deletion of pyruvate decarboxylase by a new method for efficient markerless gene deletions in *Gluconobacter oxydans*. *Appl Microbiol Biotechnol* 97(6):2521–2530
- Peters B, Mientus M, Kostner D, Junker A, Liebl W, Ehrenreich A (2013b) Characterization of membrane-bound dehydrogenases from *Gluconobacter oxydans* 621H via whole-cell activity assays using multideletion strains. *Appl Microbiol Biotechnol* 97(14):6397–6412
- Prust C, Hoffmeister M, Liesegang H, Wiezer A, Fricke WF, Ehrenreich A, Gottschalk G, Deppenmeier U (2005) Complete genome sequence of the acetic acid bacterium *Gluconobacter oxydans*. *Nat Biotechnol* 23(2):195–200
- Richhardt J, Bringer S, Bott M (2012) Mutational analysis of the pentose phosphate and Entner-Doudoroff pathways in *Gluconobacter oxydans* reveals improved growth of a Δ edd Δ eda mutant on mannitol. *Appl Environ Microbiol* 78(19):6975–6986
- Richhardt J, Luchterhand B, Bringer S, Büchs J, Bott M (2013) Evidence for a key role of cytochrome *bo*₃ oxidase in respiratory energy metabolism of *Gluconobacter oxydans*. *J Bacteriol* 195(18):4210–4220
- Rose IA, Fung WJ, Warms JV (1990) Proton diffusion in the active site of triosephosphate isomerase. *Biochemistry* 29(18):4312–4317
- Rutherford K, Parkhill J, Crook J, Horsnell T, Rice P, Rajandream MA, Barrell B (2000) Artemis: sequence visualization and annotation. *Bioinformatics* 16(10):944–945
- Sambrook J, Fritsch E, Maniatis T (1989) Molecular cloning a laboratory manual. Cold Spring Harbor Laboratory Press, Cold Spring Harbor
- Samorski M, Muller-Newen G, Büchs J (2005) Quasi-continuous combined scattered light and fluorescence measurements: a novel measurement technique for shaken microtiter plates. *Biotechnol Bioeng* 92(1):61–68
- Schweiger P, Volland S, Deppenmeier U (2007) Overproduction and characterization of two distinct aldehyde-oxidizing enzymes from *Gluconobacter oxydans* 621H. *J Mol Microbiol Biotechnol* 13(1–3):147–155
- Staden R, Beal KF, Bonfield JK (2000) The Staden package, 1998. *Methods Mol Biol* 132:115–130
- Voss J, Ehrenreich A, Liebl W (2010) Characterization and inactivation of the membrane-bound polyol dehydrogenase in *Gluconobacter oxydans* DSM 7145 reveals a role in meso-erythritol oxidation. *Microbiology* (Reading, England)
- Wach A (1996) PCR-synthesis of marker cassettes with long flanking homology regions for gene disruptions in *S. cerevisiae*. *Yeast* 12(3):259–265